



HHS Public Access

Author manuscript

J Nanopart Res. Author manuscript; available in PMC 2016 August 01.

Published in final edited form as:

J Nanopart Res. 2015 August ; 17(336): .

Effect of Carbon Nanotubes Upon Emissions From Cutting and Sanding Carbon Fiber-Epoxy Composites

William A. Heitbrink¹ and Li-Ming Lo^{2,3}

¹LMK OSH Consulting LLC, Cincinnati, OH 45233

²Division of Applied Research and technology, National Institute for Occupational Safety and Health (NIOSH), Centers for Disease Control and Prevention (CDC), Cincinnati, Ohio 45226

Abstract

Carbon nanotubes (CNTs) are being incorporated into structural composites to enhance material strength. During fabrication or repair activities, machining nanocomposites may release CNTs into the workplace air. An experimental study was conducted to evaluate the emissions generated by cutting and sanding on three types of epoxy-composite panels: Panel A containing graphite fibers, Panel B containing graphite fibers and carbon-based mat, and Panel C containing graphite fibers, carbon-based mat, and multi-walled CNTs. Aerosol sampling was conducted with direct-reading instruments, and filter samples were collected for measuring elemental carbon (EC) and fiber concentrations. Our study results showed that cutting Panel C with a band saw did not generate detectable emissions of fibers inspected by transmission electron microscopy but did increase the particle mass, number, and EC emission concentrations by 20% to 80% compared to Panels A and B. Sanding operation performed on two Panel C resulted in fiber emission rates of 1.9×10^8 and 2.8×10^6 fibers per second (f/s), while no free aerosol fibers were detected from sanding Panels A and B containing no CNTs. These free CNT fibers may be a health concern. However, the analysis of particle and EC concentrations from these same samples cannot clearly indicate the presence of CNTs, because extraneous aerosol generation from machining the composite epoxy material increased the mass concentrations of the EC.

Keywords

nanomaterial manufacturing; airborne nanoparticles; nanoparticle characterization; engineering controls; exposure prevention

Background

During fabrication of structures from composites that contain nanomaterials, composites are subjected to common mechanical processing operations such as cutting, sanding, grinding,

³Corresponding author. LLo@cdc.gov. Tel:+1 513 841 4423. Fax: +1 513 841 4506.

Disclaimer: The findings and conclusions in this article are those of the authors and do not necessarily represent the views of the National Institute for Occupational Safety and Health (NIOSH). Mention of any company or product does not constitute endorsement by NIOSH.

Compliance with Ethical Standards

The authors declare that they have no actual or potential conflict of interest in relation to this article.

and hole drilling. These machining operations can cause the generation of very high concentrations of ultrafine aerosol that exceed 10^5 particles per cubic centimeter ($\#/cm^3$) (Bello et al. 2008; Bello et al. 2009; Bello et al. 2010; Kuhlbusch et al. 2011; Methner et al. 2012). Nano-sized tubes or fibers are released as bundles of agglomerated nanomaterials or as individual fibers (Bello et al. 2010; Cena and Peters 2011; Methner et al. 2012; Schlagenhauf et al. 2012). Machining operations can involve frictional heating that may cause the generation of ultrafine aerosol with particle sizes smaller than 100 nanometers (nm) (Stabile et al. 2013). During machining operations, nanoparticle and ultrafine aerosol releases were reportedly related to the energy transported to the surface (Gheerardyn et al. 2010). The amount of energy transported to the surface is a function of the coefficient of friction, the force vector perpendicular to the surface, and tool speed. Ultimately, the mechanical power of the machining operation is converted to heat, which can increase tool and substrate temperature (Malkin and Guo 2007). According to studies of machining operations involving carbon-reinforced composites, tool temperatures can reach 287°C – 350°C and scorch marks are observed on the test composites (Weinert and Kempmann 2004; Chang et al. 2011). In structural composites involving graphite fibers cured into epoxy resins, heat damage occurs at 280°C and thermal decomposition happens at 340°C (McShane et al. 1999). Increasing the carbon nanotube (CNT) content of an epoxy composite from 0% to 2% promoted the threshold for thermal decomposition from 339°C to 378°C (Chen et al. 2008). Temperatures in excess of 400°C are reported to cause thermal decomposition for some CNTs (Hsieh et al. 2010). Frictional heating of composites can increase surface temperatures, causing thermal decomposition of the composite matrix and/or CNTs.

CNTs reportedly cause pulmonary toxicity, fibrosis, carcinogenicity, mutagenicity, immunotoxicity, and cardiovascular toxicity (Aschberger et al. 2010; Donaldson et al. 2010; EPA 2011; Schulte et al. 2012; Castranova et al. 2013). Carbon-based nanotubes or nanofibers are biopersistent and poorly soluble. Particles with a high aspect ratio are reported to cause asbestos-like health effects, including fibrosis and mesothelioma (Schulte et al. 2012). Individual fibers are more toxic than agglomerated bundles of fibers, and fiber length affects the potency of CNTs for causing mesothelioma in animals (Castranova et al. 2013). Thin (about 50 nm) multi-walled carbon nanotubes (MWCNTs) are reportedly more toxic than thicker (about 150 nm) or tangled MWCNTs (Nagai et al. 2011). However, the relationship between health effect and fiber dimensions such as fiber diameter and length have not been established (Murashov and Howard 2011; Nagai et al. 2011; Castranova et al. 2013). Reportedly, the other health effects (e.g., cardiovascular and inflammatory reactions) occur regardless of fiber length and diameter. Based on the evidence available, International Agency for Research on Cancer Monograph Working Group agreed to classify the MWCNT-7 sample as possible carcinogenic to humans (Group 2B) (Grosse et al. 2014).

Enforceable exposure limits for CNTs have not been promulgated in the United States (OSHA 2013). Exposure limits become target exposure levels and therefore assist in decision-making about the implementation of control measures (e.g., respirator selection per the OSHA respirator standard) (OSHA 2010). Various exposure limits have been proposed. Some of the proposed exposure limits relevant to this study are listed in Table 1 (Schulte et al. 2010; van Broekhuizen et al. 2012; van Broekhuizen and Dorbeck-Jung 2013). The

NIOSH recommended exposure limit (REL) for respirable elemental carbon (EC) is 1 microgram per cubic meter ($\mu\text{g}/\text{m}^3$) as an 8-hour time-weighted average (TWA) concentration set to minimize respiratory health effects (NIOSH 2013a). The other limits in Table 1 are reportedly intended to minimize exposure and are not necessarily substantiated by toxicology (Schulte et al. 2010). These limits also include particle number concentrations and fiber concentrations (Murashov and Howard 2011).

The suggested limits listed in Table 1 are low and some of them are nonspecific; extraneous aerosol generation and ambient air pollution can affect the interpretation of measurements (Murashov and Howard 2011; van Broekhuizen et al. 2012). Particle number concentrations of $20,000 \text{ \#/cm}^3$ in urban environments are routine (Shi et al. 2001; Stanier et al. 2004; Morawska et al. 2008). Atmospheric EC concentrations were observed and estimated at a mean of $0.6 \mu\text{g}/\text{m}^3$ with a standard deviation of $0.7 \mu\text{g}/\text{m}^3$, while high EC concentrations were reported to reach $5 \mu\text{g}/\text{m}^3$ (Yu et al. 2004). Vehicular traffic in urban environments can contribute to elevated EC concentrations (Lena et al. 2002). Furthermore, process-generated aerosols can contribute to the exposure measurements (Ono-Ogasawara et al. 2009). Ultrafine aerosols reportedly have been generated by direct-fire gas heaters (Peters et al. 2006), the carbon brushes on electric motors (Szymczak et al. 2007), welding (Peters et al. 2008), and grinding (Maynard and Zimmer 2002; Peters et al. 2008). Thus, the contribution of extraneous processes and background air pollution to the measured concentration levels must be determined to evaluate compliance with the exposure limits stated in Table 1 (van Broekhuizen et al. 2012).

Characterizing emissions provides insight to identify air contaminants and the needed control strategy for common fabrication and repair activities involving nanomaterial substrates. This study was conducted to measure the emission rate of airborne particles from cutting and sanding composites containing graphite fibers or CNTs. The tested composites are being used as structural components in aviation.

Methods

Test Panels

This study was conducted to characterize the particle emissions from cutting and sanding on panels of composite material made from epoxy (977-3, Cytec Industries Inc., Woodland Park, NJ) reinforced with graphite fibers (IM7, Hexcel Corporation, Stamford, CT). The specification sheet states that the filament diameter is 5.2 micrometers (μm). The fibers are dispersed throughout all of three test panels. Specifically, three panels with dimensions 30.5×30.5 centimeters (cm) were tested:

1. Panel A: This panel consists of IM7 graphite fiber in a cured epoxy resin.
2. Panel B: This panel has the same basic composition as Panel A but with a carbon-based nonwoven mat as a surface ply. The mat has a fiber diameter of $7.5 \mu\text{m}$.
3. Panel C: This panel has the same basic composition as Panel B. However, the mat is coated with M-grade MWCNTs (Buckeye Composites, Kettering, OH) and a

binder. The M-grade MWCNTs have an average diameter of 50 nm and an average length of 1 millimeter (mm).

Sampling System

Ventilated Enclosure—An enclosing hood (Figure 1) was constructed to capture the dust generated by cutting and sanding the composite panels. The aerosol was transported to the sampling location through a ventilation duct (Figure 2). Emission concentrations or rates were estimated as the product of air flow and contaminant mass concentrations. The enclosure around the band saw, shown in Figure 3, was constructed from 3.175-cm inner diameter polyvinyl chloride (PVC) pipes and 6-mil polyethylene vapor barrier. The enclosure included a mixing baffle between the air distribution slots and the exit from the enclosure. To create turbulence to mix the aerosol, two 2.54- × 96-cm slots were cut out of the mixing baffle about 4 cm from the side.

This test system was intended to promote mixing so that a single point would be a representative sample of the aerosol in the duct. The space between the baffle and the connection to the 30.5-cm-diameter duct (see Figure 1) should cause the formation of large-scale eddies that cause mixing (McFarland et al. 1999). Elbows also promote turbulence and mixing. The sampling location was 15 duct-diameters downstream of the elbow (see Figure 2), which should adequately mix the aerosol (Hampl et al. 1986)

As shown in Figure 2, the branch connection just upstream of the portable air exhaust system (Novair 2000, Novatek Co., Exton, PA) combined air from the duct system and a 20-cm branch to which an adjustable blast gate was attached. The procedures outlined in the Ventilation Manual was followed to measure the air flow in the duct by two 10-point Pitot tube traverses horizontally and vertically (ACGIH 2013). The blast gate was placed on this connection to obtain the desired ventilation parameters; it was adjusted to keep the air velocity near the sampling nozzles for the Aerodynamic Particle Sizer (APS) and integrated filter samples at the desired 7 m/s as measured by the hot wire anemometer (VelociCalc Plus model 8386A, TSI Inc., Shoreview, MN).

In-Duct Sampling—Because particles smaller than 0.5 μm have negligible inertia, the FMPS drew sampled air by inserting a hose into the duct at the location shown in Figure 2. However, particle inertia can affect inlet sampling efficiency for larger particles. The APS and integrated samples were collected through isokinetic nozzles that were fabricated from brass shim stock (0.03 cm thickness) and sized for a duct velocity of 7 meters per second (m/s). The nozzle for the APS had an inlet diameter of 0.39 cm and a length of 5 cm; the nozzles for the integrated samples had an inlet diameter of 0.35 cm and a length of 3.3 cm.

The nozzle for the APS sampling was fitted into the copper tubing with an inside diameter of 1.92 cm, but the nozzle for the filter samples was compressed into the middle ring of an open-faced 25-mm filter. The entire nozzle assembly was soldered together. A tubing or conduit bender was used to create a gradual 90° bend so that the ratio of the radius of the bend to the tubing diameter (R/D) was 5.7, and the tubing Reynolds number (Re) was 353.

Gravitational settling losses in the nozzles are unavoidable. Aerosol penetrations through the nozzles (transmission efficiency) for particles of 1, 5, and 10 μm were estimated (Brockman 2011) and summarized in Table 2. The overall transmission efficiency through an elbow at R/D of 5.7 and Re of 1,000 was reportedly better than 0.95 (Brockman 2011). Therefore, the losses of particles smaller than 10 μm from the APS sampling should be negligible.

Direct-Reading Aerosol Measurements—In the nano-manufacturing workplace, direct-reading instruments used in real-time mode can help identify major emission sources and to assess the efficiency of control measures. They provide continuous measurements of concentrations that can be correlated with the specific production equipment and work processes (Ham et al. 2012). Size-dependent particle number concentrations were measured with the following two instruments:

1. The Fast Mobility Particle Sizer (FMPS) (Model 3091, TSI Inc., Shoreview, MN) uses an array of 32 electrometers to measure electrical mobility diameters between 5.6 and 560 nm. For a 1-second sample, the detectable number concentration is from 100 to 10^7 $\#/\text{cm}^3$ at 5.6 nm and 1 to 10^5 $\#/\text{cm}^3$ at 560 nm.
2. The Aerodynamic Particle Sizer (APS) (Model 3320, TSI Inc., Shoreview, MN) uses particle transit time in an accelerating air flow to measure equivalent optical sizes between 0.5 and 20 μm . Its maximum processing rate for aerodynamic sizing is larger than 200,000 $\#/\text{cm}^3$.

The APS and the FMPS were used exclusively for in-duct sampling. Both instruments provide number concentrations expressed as $\#/\text{cm}^3$. Assuming that the aerosol particles are spherical with a density (ρ) of 1 g/cm^3 , mass concentrations can be estimated by the following equation.

$$C_m = \sum_{i=1}^j \frac{\pi}{6} d_{p,i}^3 \rho C_{n,i} \quad (1)$$

where

C_m = mass concentration, mg/m^3 ,

$d_{p,i}$ = midpoint particle diameter, μm , and

$C_{n,i}$ = number concentration at the instrument channel i of j channels, $\#/\text{cm}^3$.

The respirable mass of aerosol (C_{resp}) in channel i can be computed by multiplying $C_{m,i}$ by the fractional amount of respirable aerosol ($f_{resp,i}$) that is documented in Appendix C of ACGIH's listing of threshold limit values for chemical substances (ACGIH 2012).

$$C_{resp} = \sum_{i=1}^j \frac{\pi}{6} d_{p,i}^3 \rho f_{resp,i} C_{n,i} \quad (2)$$

All of the mass emissions measured by the FMPS were assumed to be respirable. For the APS data, the mass fraction of respirable aerosol was computed as C_{resp}/C_m .

Before data collection, the times on all of the computers and instruments were synchronized. Data collection occurred on 2 days. At the start of each day, background samples for EC and fibers were collected behind the test enclosure. This location was about 10 m from the discharge of the air exhaust system and near the back of the enclosure. These samples quantify the ambient concentrations that were present in the study site.

Integrated Filter Samples

Air samples to determine the airborne mass concentration of EC were collected on open-face quartz fiber filters using air pumps (Universal Aircheck Sampler, Model 224-PCXR, SKC Inc., Eight Four, PA) at a sampling rate of 4 liters per minute (L/min). These 25-mm diameter filter samples were analyzed according to NIOSH NMAM 5040 (NIOSH 2003). In this study, seven media blanks were processed to determine the limit of detection (LOD) and limit of quantitation (LOQ).

Alongside each mass-based air sample, additional air samples were collected on 25-mm diameter, open-face mixed cellulose ester filters for CNT/fiber inspection using TEM with energy dispersive spectroscopy (EDS) in a manner similar to NIOSH NMAM 7402 (NIOSH 1994). These samples were also collected with SKC air pumps operated at 4 L/min. Three 3-mm copper TEM grids from each sample were examined at low magnification to determine loading and preparation quality. The counting protocol was every 40 grid openings or 100 structures. TEM with EDS provides an indication of the relative abundance of nanostructures per cm^3 of air, as well as other characteristics such as size, shape, chemical composition, and degree of agglomeration.

The filter samples for EC and fiber concentration were collected in the duct, on the worker, in the enclosure just downstream of the sanding or sawing operation (i.e., source samples), and at a background location. The duct samples were taken at the location shown in Figure 2 using sampling nozzles to obtain isokinetic sampling conditions. The source sample was taken just behind the band saw's table (Figure 3) to help characterize the emissions. The background sample was taken during each day of the study. The samples collected on the worker were used to evaluate the extent to which air contaminants can leak from the enclosure. Because the EC samples were not respirable samples, the results cannot be used to evaluate compliance with the exposure limits for CNTs stated in Table 1.

Machining Operations

In this study, cutting and sanding operations for test panels were tested to evaluate the emissions of nanomaterials due to these common fabrication and repair processes for nanocomposites.

Panel Cutting—A vertical band saw (Model 20, Delta Power Equipment Co., Anderson County, SC) was used to cut the composite panels (Figure 3). The band saw blade was located about 35 cm inside the enclosure. This band saw had a nominal blade speed of 25.9 m/s. It was used with a 3.84-m long and 0.0762-cm thick blade. The same blade was used for all tests of panel cutting.

Before using the band saw to cut composites, the aerosol emissions from the band saw were characterized by operating it for a period of 10 minutes without cutting. Next, each test panel was cut in half and one half-panel from each sample was reserved for the sanding experiments. Then, the other half of the panel was repeatedly cut using the band saw, resulting in 15-cm-long pieces of composite, which were discarded. The concentrations from the first cut of each panel were used to estimate the number of cuts for the test panels to generate the same mass loading on filter samples for transmission electron microscopy (TEM) analysis. Therefore, eleven cuts were made on Panel A, 11 cuts on Panel B, and 5 cuts on Panel C. Because of a short time needed for making a single cutting, the worker continued the cutting process on each test panel for filter sampling. The sampling pumps were turned on a few seconds before cutting the panels and off about 1 minute after the cutting had stopped to allow the pulse of particle emissions to pass the in-duct aerosol instrumentation.

Panel Sanding—For the sanding experiments, the sander (Model S652D, Ryobi, Hiroshima-Ken, Japan, Figure 4) with fresh sand paper was used to sand the 30.5- × 15-cm composite panels (Panel A, Panel B, and Panel C1). A second test panel of composite C (Panel C2) became available during the sanding tests, and it was also cut to the test size and sanded. The sand paper was 100-grit with holes punched in the sand paper using the tool provided with the sander. The worker conducted the sanding operation on the work table of the band saw machine. The sanding operation was stopped once the substrate of the test panel was observed. The start and stop times for the sanding were recorded and used to estimate the emission rate. The actual sampling time was about 1 minute longer to allow the pulse of higher particle concentration to pass the sampling instruments in the duct.

After conducting the testing, we learned that the sander contained carbon brushes, which are reported to be a source of extraneous aerosol generation (Trakumas et al. 2001; Heitbrink and Collingwood 2005; Szymczak et al. 2007; Koponen et al. 2009). In electric motors, carbon brushes, which are essentially sticks or blocks of graphite, rub against the rotating commutator to complete the tool's power circuit. This inevitably creates dust due to abrasion and, perhaps, arcing. The heat and aerosol are discharged through ventilation holes in the sander's handle. To evaluate the emissions from the sander itself, the exhaust duct/air cleaner set-up (Figure 2) was reassembled in our ventilation lab after the experimental tests conducted at the site. The sander was positioned in an elbow (Figure 4) so that the aerosol generated by the sander was captured. The enclosure around the band saw was not reconstructed for these lab tests. This lab is air-conditioned and the supplied air passes through minimum efficiency reporting value (MERV) 12 filters to maintain low background concentrations.

Data Analysis

For composite cutting, the results are presented as emission concentrations (EM). To compute the EM , the concentration increase, C , is determined as the difference between the in-duct concentration during the sampling time and the average concentration measured before the composite was cut (i.e., 5 minutes background concentration measured near the back of the enclosure in this study). The panel thicknesses and cut lengths varied so that

concentrations were not directly comparable. To remedy this, the EM was normalized based upon the volume of composite cut (V_c), air flow (Q), and sampling time (t). Therefore, emission concentrations from the process of composite cutting can be determined by:

$$EM = \frac{\Delta C Q t}{V_c} \quad (3)$$

where

EM = emission concentration, $\#/cm^3$ (for small particles from FMPS data) and mg/cm^3 (for large particles from APS data),

C = concentration increase, $\#/cm^3$ or mg/cm^3 same as EM ,

Q = air flow rate, cm^3/s ,

t = sampling time, s, and

V_c = (blade thickness) \times (length of cut) \times (panel thickness), cm^3 . The values of V_c are presented in Table 3.

Unlike the cutting process where large volumes of materials were removed from the test panels, the emission rate (ER) for composite sanding is based upon the sanding time. The concentrations are determined by the actual sampling time. Emission rates from the sanding process were computed by:

$$ER = \frac{\Delta C Q t}{t_s} \quad (4)$$

where

ER = emission rate, $\#/s$ (for small particles from FMPS data) and mg/s (for large particles from APS data), and

t_s = sanding time, s.

Results

Ventilation Measurements

The ventilation measurements were made to control airflow in the test system. The hood face velocity at the inlet was 1 m/s. The average centerline duct velocity near the sample probes was set to 7 m/s, and the exhaust air flow was 0.5 m^3/s . Flow visualization with smoke tubes did not reveal the presence of eddies that might transport air contaminants out of the hood. In general, the particle emissions from test processes should have been contained within the test system.

Cutting Process

As shown in Table 4, cutting the panels with a band saw generated very high particle number concentrations (between 480,000 and 730,000 $\#/cm^3$). Panel C had a particle number emission concentration that was 20% higher than Panel A and 53% higher than Panel B. For the number size distribution, Panel A had a smaller size (nominal mode of 10 nm) than Panels B and C (modes at about 35–40 nm) (Figure 5a). The possible reason for

this size difference was that Panels B and C were synthesized to enhance their mechanical strength—Panel B with a nonwoven mat and Panel C with MWCNTs. As shown in Table 4, the mass emission concentration for Panel C was 73 % higher than Panel A and 80% higher than Panel B. The shape of the mass distribution was not affected by the inclusion of the CNTs as the size distributions had a mode of 4–5 μm (Figure 5b). About half of the aerosol mass measured with APS was respirable as shown on the results of C_{resp}/C_m .

The EC concentrations are presented in Table 5. The EC concentrations at the source during cutting of Panel B ($93 \mu\text{g}/\text{m}^3$) can be as high as 50 times the background concentration ($1.8 \mu\text{g}/\text{m}^3$). The lowest EC concentration was found from Panel A ($35 \mu\text{g}/\text{m}^3$), but it was at least 20 times higher than the background. This demonstrated that fragments of the larger carbon and graphite fibers were contributing to the EC concentration. The EC emission concentration was $6.9 \text{ mg}/\text{cm}^3$ of cut volume for Panel C versus $4.9 \text{ mg}/\text{cm}^3$ for Panels A and $4.1 \text{ mg}/\text{cm}^3$ for Panel B. However, CNTs or fibers were not detected on any of the samples collected in the duct, on the worker, or at the source. Apparently, the EC measurements were not necessarily indicative of nanomaterial exposure in this case.

The EC concentrations measured on the worker were less than $1 \mu\text{g}/\text{m}^3$ for all three test panels and they were less than the background measured in the plant (Table 5). The concentrations measured on the worker were less than 1% of the concentrations measured in the duct. The hood appeared to be effective at reducing exposure for the band saw operator.

Sanding Process

As reported in Table 6, particle number concentrations during panel sanding were between 15,000 and 18,000 $\#/\text{cm}^3$, compared with the background aerosol concentration at 11,000 $\#/\text{cm}^3$. The in-duct sampling system excluding the test enclosure was reassembled in the laboratory to evaluate the sander operation; the concentration increase caused by the sander alone was 4,500 $\#/\text{cm}^3$, compared with the laboratory background concentration, which was under 150 $\#/\text{cm}^3$. Expressed as an emission rate, the sander produced 2×10^9 $\#/\text{s}$ based on the adjusted flow rate. The range of observed emissions from sanding the panels in the study site was from 10^9 to 4.3×10^9 $\#/\text{s}$. The sander accounts for approximately 46% to 100% of the particle emissions. The plot of emission rate as a function of particle size in Figure 6a also shows that the sander itself contributes most of the particles smaller than about 15 nm. For particles larger than 50 nm, no measured emissions were from the sander alone, while the sanding operation generated a noticeable number of particles.

Table 6 and Figure 6b present the mass emission rates. As shown in Figure 6b, the mode in the mass distribution is between 3 and 4 μm . Panels B and C1 produced mass emission rates of 0.32 and 0.36 mg/s , but the mass emission rate for Panel A was 0.04 mg/s and Panel C2 was 0.02 mg/s . The reason for the observed emission rate difference is not known. However, no mechanism existed to control the force applied to the sander, and this can affect the frictional force between the surface and the sander (Ringlein and Robbins 2004; Gheerardyn et al. 2010). According the APS data (Table 6), the range of mass fractions of respirable aerosol (C_{resp}/C_m) from sanding test panels was from 0.58 to 0.64.

The TEM results are summarized in Table 7. Fibers were detected only when Panels C1 and C2 were sanded, but they were not detected on the personal samples. The fiber number concentrations in the duct were 290 fibers per cubic meter (f/cm^3) for Panel C1 and $4.3 f/cm^3$ for Panel C2; the emission rates were $1.9 \times 10^8 f/s$ for Panel C1 and $2.8 \times 10^6 f/s$ for Panel C2. As shown in Figure 7, these fibers had a length shorter than $5 \mu m$, which is the length specified for asbestos fibers in occupational exposure limits (ACGIH 2012). The CNTs and fibers used for toxicological testing were typically reported to be fiber bundles (Murray et al. 2012). In our study, the released fibers mostly existed individually (Figure 7a c and 7e). However, some fibers protruded from the particles (Figure 7d and 7f). The extent to which this fiber concentration and emission rate pose a hazard is unclear as the relationship between CNT shape (e.g., diameter, length, bundle size) and health hazard is not known.

The EC concentrations measured during the sanding operations appeared to be minimal (Table 8). A background sample collected for EC analysis during all of the sanding operations was $0.1 \mu g/m^3$. The EC emission rate during sanding of Panel A was $1.63 \mu g/s$ and Panel C1 was $2.51 \mu g/s$, both higher than those for Panels B and C2. These EC results were different from the TEM data (Table 7) indicating that fiber emissions found from Panels C1 and C2 but not from Panels A and B. The possible reason of no correlation between the EC measurement and the observed fibers is due to different top coating materials on each test panels: Panel A with graphite fibers, Panel B with a nonwoven mat, and Panels C1 and C2 with MWCNTs. The concentrations measured in the worker breathing zone were below the NIOSH REL for CNTs of $1 \mu g/m^3$ measured as respirable EC, except for Panel B ($1.62 \mu g/m^3$). The higher EC concentration generated from sanding Panel B could be due to its softer surface coating. Panel B was thicker than other test panels (Table 3) but its surface was removed more easily than others. However, the induct sampling did not show consistent high EC concentrations from sanding Panel B. Again, the EC from the graphite fibers may be contributing to the EC concentrations and obscuring the EC concentrations resulting from the CNTs.

Discussion

The available data generally support the conclusion that the ventilated enclosure efficiently captured the debris generated by cutting and sanding the composite panels. Thus the emissions were completely captured enabling a characterization of emissions from machining nanocomposites. Flow visualization suggested that the ventilation system was separating the worker from the aerosol generated within the enclosure. The aerosol measurement also showed that worker exposure was not different than background air pollution, and the concentration measured on the worker was much less than the concentration in the duct.

To compare measurements with suggested exposure limits for engineered nanomaterials (e.g., Table 1), it is necessary to evaluate whether exposure measurements are due to engineered nanomaterials or extraneous aerosol sources (van Broekhuizen and Dorbeck-Jung 2013). As identified by TEM data, the number concentration of CNTs from panel sanding was less than $290 f/cm^3$. In contrast, the number concentration of aerosol

generated by the sander was about 4.5×10^3 particles/cm³; likely from the motor's carbon brushes. Furthermore, the fiber concentration was much lower than the number concentration measured by FMPS reported in Table 4 and Table 6. Although number concentrations generated during band saw cutting were 10^5 to 10^6 particles/cm³ (Table 4) and EC concentrations were 50 to 84 µg/m³ (Table 5), TEM data did not reveal the presence of CNTs or any fibers. For cutting with the band saw, the observed concentrations of extraneous aerosol and EC were much higher than the provisional occupational exposure limits stated in Table 1. In this study, TEM analysis seemed a better tool to identify real concentrations of nanomaterials. Clearly, one needs to consider the extent to which measuring concentrations are actually nanomaterials for characterizing worker exposures.

Sanding the composite Panel C, which contained CNTs, generated measurable fiber concentrations. The extent of the hazard is not known as relevant exposure metrics have not been developed. However, careful and aggressive control of exposure to CNTs is recommended (Castranova et al. 2013). The enclosure used in this study effectively contained the emissions, but it may not be suitable for all applications. The band saw used in this study had an exhaust take-off that could be attached to a vacuum cleaner; however, air flow recommendations are not available. The ACGIH Ventilation Manual has ventilation recommendations for band saws (ACGIH 2013). Orbital sanders frequently have exhaust take-offs for drawing air through holes in the sanding pads and sand paper. For orbital sanders, an exhaust flow rate of 1 m³/min can provide a 90% reduction in emissions when an appropriate vacuum cleaner is used to provide airflow and dust collection (Thorpe and Brown 1994, 1995). The dust collection bags provided with sanders and vacuum cleaners may be ineffective as dust control measures and in providing adequate airflow and air cleaning. In using vacuum cleaners, air flow maintenance needs to be addressed as some vacuum cleaners lose noticeable amounts of air flow as debris accumulates in the vacuum cleaner (Heitbrink and Santalla-Elias 2009). In addition to ventilation, water can sometimes be used to suppress dust generation. However, this requires efforts to develop application methods and to address electrical safety issues.

Conclusions

Sanding composites containing CNTs released fiber emissions while cutting these composites on a band saw did not generate noticeable quantities of fiber emissions. Both operations produced emissions of EC and ultrafine particles that are not specific to CNTs. The tested composites contained graphite and carbon fibers that caused most of the measured emissions of EC. Cutting on the band saw created extremely high ultrafine aerosol number concentrations. The sander motor appeared to generate large quantities of ultrafine aerosol. Adjusting exposure measurements for these extraneous aerosol sources would involve large adjustments that may obscure and overwhelm exposures that are excessive in terms of draft or provisional exposure limits for CNTs. Use of the EC mass data to determine possible occupational exposure to CNTs needs to be verified with TEM since other sources of EC (such as carbon composites) can contribute to the mass loading. According to the documentation for the NIOSH REL, other potential EC exposures may interfere with the interpretation of worker CNT exposure (NIOSH 2013a). Clearly, the hood used in this study effectively contained the emissions, but this enclosure may not be suitable

in all applications. Local exhaust ventilation can be used to capture and collect the aerosol and debris generated by the band saw. Useful information for controlling fugitive nanomaterials in the workplace is available from some published documents (SWA 2009; HSE 2011; ISO 2013; NIOSH 2013b).

Acknowledgments

The authors would like to acknowledge the support and cooperation from the management and the staff of the study site, and wish to thank Alberto Garcia for his assistance with field study. The authors are grateful to Laura Hodson, Arthur Miller, Appavoo Rengasamy, Jennifer Topmiller, Michael Gressel, and Cathy Rotunda for their insightful comments and suggestions on the early version of the manuscript. This research was funded by the National Institute for Occupational Safety and Health under the Nanotechnology Research Center project 927ZJLR.

References

- ACGIH. TLVs and BEIs: threshold limit values for chemical substances and physical agents and biological exposure indices. American Conference of Governmental Industrial Hygienists; Cincinnati, OH: 2012.
- ACGIH. Industrial ventilation: a manual of recommended practice for design. American Conference of Governmental Industrial Hygienists; Cincinnati, Ohio: 2013.
- Aschberger K, Johnston HJ, Stone V, Aitken RJ, Hankin SM, Peters SAK, Tran CL, Christensen FM. Review of carbon nanotubes toxicity and exposure-appraisal of human health risk assessment based on open literature. *Crit Rev Toxicol*. 2010; 40 (9):759–790. [PubMed: 20860524]
- Bello D, Hart AJ, Ahn K, Hallock M, Yamamoto N, Garcia EJ, Ellenbecker MJ, Wardle BL. Particle exposure levels during CVD growth and subsequent handling of vertically-aligned carbon nanotube films. *Carbon*. 2008; 46 (6):974–977.
- Bello D, Wardle B, Zhang J, Yamamoto N, Santeufemio C, Hallock M, Virji MA. Characterization of exposures to nanoscale particles and fibers during solid core drilling of hybrid carbon nanotube advanced composites. *Int J Occup Environ Health*. 2010; 16 (4):434–450. [PubMed: 21222387]
- Bello D, Wardle BL, Yamamoto N, Guzman deVilloria R, Garcia EJ, Hart AJ, Ahn K, Ellenbecker MJ, Hallock M. Exposure to nanoscale particles and fibers during machining of hybrid advanced composites containing carbon nanotubes. *J Nanopart Res*. 2009; 11 (1):231–249.
- Brockman, JE. Aerosol transport in sampling lines and inlets. In: Kulkarni, P.; Baron, PA.; Willeke, K., editors. *Aerosol measurement: principles, techniques, and applications*. 3. John Wiley & Sons Inc; Hoboken, NJ: 2011. p. 69-105.
- Castranova V, Schulte PA, Zumwalde RD. Occupational nanosafety considerations for carbon nanotubes and carbon nanofibers. *Accounts Chem Res*. 2013; 46 (3):642–649.
- Cena LG, Peters TM. Characterization and control of airborne particles emitted during production of epoxy/carbon nanotube nanocomposites. *J Occup Environ Hyg*. 2011; 8 (2):86–92. [PubMed: 21253981]
- Chang CS, Ho JE, Chan CH, Hwang BC. Prediction of cutting temperatures in turning carbon fiber reinforced plastics composites with worn tools. *J App Sci*. 2011; 11:3698–3707.
- Chen X, Wang J, Lin M, Zhong W, Feng T, Chen X, Chen J, Xue F. Mechanical and thermal properties of epoxy nanocomposites reinforced with amino-functionalized multi-walled carbon nanotubes. *Mater Sci Eng A*. 2008; 492 (1–2):236–242.
- Donaldson K, Murphy FA, Duffin R, Poland CA. Asbestos, carbon nanotubes and the pleural mesothelium: a review of the hypothesis regarding the role of long fibre retention in the parietal pleura, inflammation and mesothelioma. *Part Fibre Toxicol*. 2010; 7(5)
- EPA. Control of nanoscale materials under the Toxic Substances Control Act. U.S. Environmental Protection Agency; 2011. <http://www.epa.gov/oppt/nano/> [Accessed April 3 2014]
- Gheerardyn, L.; Le Bihan, O.; Dore, E.; Morgeneyer, M. Nanoparticle release from nano-containing product, introduction to an energetic approach. Paper presented at the Nanotechnology Conference & Expo; 2010; Anaheim, CA. 2010.

- Grosse, Y.; Loomis, D.; Guyton, KZ.; Lauby-Secretan, B.; El Ghissassi, F.; Bouvard, V.; Benbrahim-Tallaa, L.; Guha, N.; Scoccianti, C.; Mattock, H.; Straif, K. Carcinogenicity of fluoro-edenite, silicon carbide fibres and whiskers, and carbon nanotubes. *The Lancet Oncology*. 2014. [http://dx.doi.org/10.1016/S1470-2045\(14\)71109-X](http://dx.doi.org/10.1016/S1470-2045(14)71109-X)
- Ham S, Yoon C, Lee E, Lee K, Park D, Chung E, Kim P, Lee B. Task-based exposure assessment of nanoparticles in the workplace. *J Nanopart Res*. 2012; 14 (9):1–17. [PubMed: 22448125]
- HAMPL V, Niemelä R, Shulman S, Bartley DL. Use of tracer gas technique for industrial exhaust hood efficiency evaluation—where to sample? *Am Ind Hyg Assoc J*. 1986; 47 (5):281–287. [PubMed: 3717012]
- Heitbrink WA, Collingwood S. Aerosol generation by blower motors as a bias in assessing aerosol penetration into cabin filtration systems. *J Occup Environ Hyg*. 2005; 2 (1):45–53. [PubMed: 15764523]
- Heitbrink WA, Santalla-Elias J. The effect of debris accumulation on and filter resistance to airflow for four commercially available vacuum cleaners. *J Occup Environ Hyg*. 2009; 6 (6):374–384. [PubMed: 19360515]
- HSE. Controlling airborne contaminants at work: a guide to local exhaust ventilation (LEV). Health and Safety Executive; UK: 2011. Series code HSG258
- Hsieh YC, Chou YC, Lin CP, Hsieh TF, Shu CM. Thermal analysis of multi-walled carbon nanotubes by Kissinger's corrected kinetic equation. *Aerosol Air Qual Res*. 2010; 10 (3):212–218.
- ISO. Nanotechnologies -- guidelines for occupational risk management applied to engineered nanomaterials -- Par2: the use of the control banding approach in occupational risk management. International Organization of Standardization; Geneva, Switzerland: 2013. ISO/PDTS 12901-2
- Koponen I, Jensen K, Schneider T. Sanding dust from nanoparticle-containing paints: physical characterisation. *J Phys: Conf Ser*. 2009; 151 (1):012048.
- Kuhlbusch TAJ, Asbach C, Fissan H, Gohler D, Stintz M. Nanoparticle exposure at nanotechnology workplaces: a review. *Part Fibre Toxicol*. 2011; 8:22. [PubMed: 21794132]
- Lena TS, Ochieng V, Carter M, Holguín-Veras J, Kinney PL. Elemental carbon and PM (2.5) levels in an urban community heavily impacted by truck traffic. *Environ Health Perspect*. 2002; 110 (10): 1009. [PubMed: 12361926]
- Malkin S, Guo C. Thermal analysis of grinding. *CIRP Ann-Manuf Technol*. 2007; 56 (2):760–782.
- Maynard A, Zimmer A. Evaluation of grinding aerosols in terms of alveolar dose: the significance of using mass, surface area and number metrics. *Ann Occup Hyg*. 2002; 46 (suppl 1):315–319.
- McFarland AR, Gupta R, Anand N. Suitability of air sampling locations downstream of bends and static mixing elements. *Health Phys*. 1999; 77 (6):703–712. [PubMed: 10568550]
- McShane, H.; Arafat, ES.; McLaughlin, P.; Cochran, R.; Miller, K.; Arnold, F.; Cramer, R. Heat damage assessment for Naval aircraft composites. Naval Air Warfare Center Aircraft Division Patuxent River; MD: 1999.
- Methner M, Crawford C, Geraci C. Evaluation of the potential airborne release of carbon nanofibers during the preparation, grinding, and cutting of epoxy-based nanocomposite material. *J Occup Environ Hyg*. 2012; 9 (5):308–318. [PubMed: 22545869]
- Morawska L, Ristovski Z, Jayaratne E, Keogh DU, Ling X. Ambient nano and ultrafine particles from motor vehicle emissions: characteristics, ambient processing and implications on human exposure. *Atmos Environ*. 2008; 42 (35):8113–8138.
- Murashov, V.; Howard, J. Nanotechnology standards. New York: 2011. Health and safety standards; p. 209-238.
- Murray AR, Kisin ER, Tkach AV, Yanamala N, Mercer R, Young SH, Fadeel B, Kagan VE, Shvedova AA. Factoring-in agglomeration of carbon nanotubes and nanofibers for better prediction of their toxicity versus asbestos. *Part Fibre Toxicol*. 2012; 9 (1):10. [PubMed: 22490147]
- Nagai H, Okazaki Y, Chew SH, Misawa N, Yamashita Y, Akatsuka S, Ishihara T, Yamashita K, Yoshikawa Y, Yasui H. Diameter and rigidity of multiwalled carbon nanotubes are critical factors in mesothelial injury and carcinogenesis. *Proceedings of the National Academy of Sciences*. 2011; 108 (49):E1330–E1338.

- NIOSH. Asbestos by TEM, Method 7402. U.S. Department of Health and Human Services, Centers for Disease Control and Prevention, National Institute for Occupational Safety and Health; Cincinnati, OH: 1994.
- NIOSH. Diesel particulate matter (as elemental carbon), Method 5040. U.S. Department of Health and Human Services, Centers for Disease Control and Prevention, National Institute for Occupational Safety and Health; Cincinnati, OH: 2003.
- NIOSH. Current intelligence bulletin 65: occupational exposure to carbon nanotubes and nanofibers. U.S. Department of Health and Human Services, Centers for Disease Control and Prevention, National Institute for Occupational Safety and Health; Cincinnati, OH: 2013a. DHHS (NIOSH) Publication No. 2013-145
- NIOSH. Current strategies for engineering controls in nanomaterial production and downstream handling processes. U.S. Department of Health and Human Services, Centers for Disease Control and Prevention, National Institute for Occupational Safety and Health; Cincinnati, OH: 2013b. DHHS (NIOSH) Publication No. 2014-102
- Ono-Ogasawara M, Serita F, Takaya M. Distinguishing nanomaterial particles from background airborne particulate matter for quantitative exposure assessment. *J Nanopart Res.* 2009; 11 (7): 1651-1659.
- OSHA. Respiratory protection, 29CFR1910.134. Occupational Safety and Health Administration; Washington, DC: 2010.
- OSHA. OSHA Fact sheet: working safely with nanomaterials, DTSEM FS-3634 01/2013. Occupational Safety and Health Administration; Washington, DC: 2013.
- Peters TM, Elzey S, Johnson R, Park H, Grassian VH, Maher T, O'Shaughnessy P. Airborne monitoring to distinguish engineered nanomaterials from incidental particles for environmental health and safety. *J Occup Environ Hyg.* 2008; 6 (2):73-81. [PubMed: 19034793]
- Peters TM, Heitbrink WA, Evans DE, Slavin TJ, Maynard AD. The mapping of fine and ultrafine particle concentrations in an engine machining and assembly facility. *Ann Occup Hyg.* 2006; 50 (3):249-257. [PubMed: 16361396]
- Ringlein J, Robbins MO. Understanding and illustrating the atomic origins of friction. *Am J Phys.* 2004; 72 (7):884-891.
- Schlagenhauf L, Chu BT, Buha J, Nuesch F, Wang J. Release of carbon nanotubes from an epoxy-based nanocomposite during an abrasion process. *Environ Sci Tech.* 2012; 46 (13):7366-7372.
- Schulte P, Murashov V, Zumwalde R, Kuempel E, Geraci C. Occupational exposure limits for nanomaterials: state of the art. *J Nanopart Res.* 2010; 12 (6):1971-1987.
- Schulte PA, Kuempel ED, Zumwalde RD, Geraci CL, Schubauer-Berigan MK, Castranova V, Hodson L, Murashov V, Dahm MM, Ellenbecker M. Focused actions to protect carbon nanotube workers. *Am J Ind Med.* 2012; 55 (5):395-411. [PubMed: 22392774]
- Shi JP, Evans DE, Khan AA, Harrison RM. Sources and concentration of nanoparticles (<10nm diameter) in the urban atmosphere. *Atmos Environ.* 2001; 35 (7):1193-1202.
- Stabile L, Ruggiero A, Iannitti G, Buonanno G. Generation of ultrafine particles by high-velocity impact of metal projectiles on a metallic target. *J Aerosol Sci.* 2013; 55:66-77.
- Stanier CO, Khlystov AY, Pandis SN. Ambient aerosol size distributions and number concentrations measured during the Pittsburgh Air Quality Study (PAQS). *Atmos Environ.* 2004; 38 (20):3275-3284.
- SWA. Engineered nanomaterials: evidence on the effectiveness of workplace controls to prevent exposure. Safe Work Australia; Braddon, Australia: 2009.
- Szymczak W, Menzel N, Keck L. Emission of ultrafine copper particles by universal motors controlled by phase angle modulation. *J Aerosol Sci.* 2007; 38 (5):520-531.
- Thorpe A, Brown R. Measurements of the effectiveness of dust extraction systems of hand sanders used on wood. *Ann Occup Hyg.* 1994; 38 (3):279-302. [PubMed: 8048789]
- Thorpe A, Brown R. An improved design for the dust extraction system of orbital sanders used on wood. *Ann Occup Hyg.* 1995; 39 (2):155-165.
- Trakumas S, Willeke K, Grinshpun SA, Reponen T, Mainelis G, Friedman W. Particle emission characteristics of filter-equipped vacuum cleaners. *AIHAJ.* 2001; 62 (4):482-493. [PubMed: 11549143]

- van Broekhuizen P, Dorbeck-Jung B. Exposure limit values for nanomaterials -- capacity and willingness of users to apply a precautionary approach. *J Occup Environ Hyg.* 2013; 10 (1):46–53. [PubMed: 23216200]
- van Broekhuizen P, van Veelen W, Streeckstra WH, Schulte P, Reijnders L. Exposure limits for nanoparticles: report of an international workshop on nano reference values. *Ann Occupa Hyg.* 2012; 56 (5):515–524.
- Weinert K, Kempmann C. Cutting temperatures and their effects on the machining behaviour in drilling reinforced plastic composites. *Adv Eng Mater.* 2004; 6 (8):684–689.
- Yu S, Dennis RL, Bhave PV, Eder BK. Primary and secondary organic aerosols over the United States: estimates on the basis of observed organic carbon (OC) and elemental carbon (EC), and air quality modeled primary OC/EC ratios. *Atmos Environ.* 2004; 38:5257–5268.

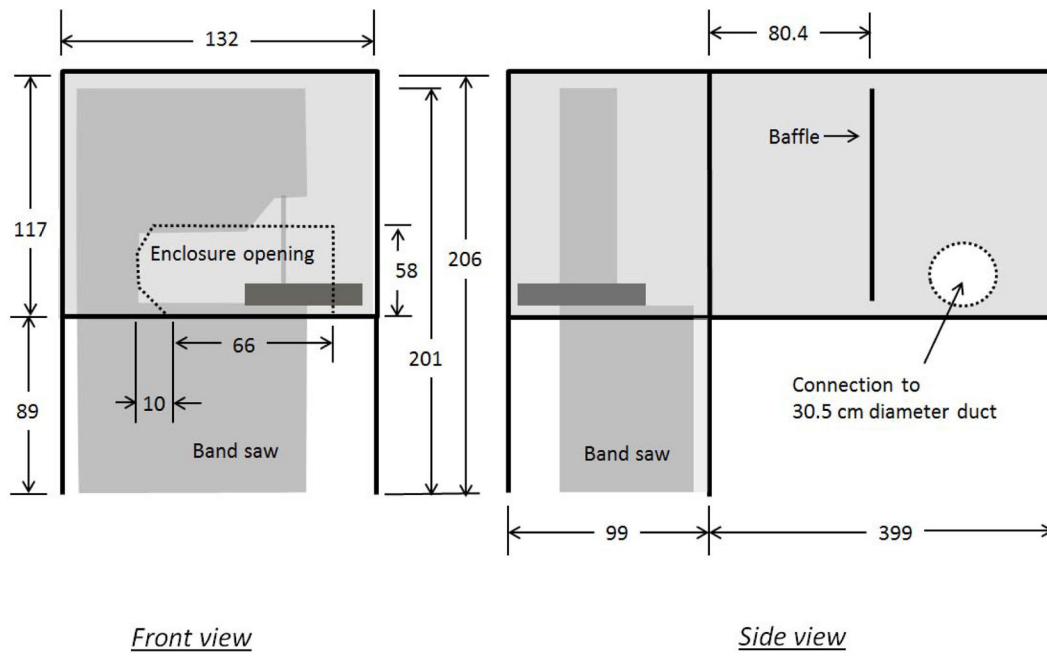


Figure 1. Front and side views of the enclosure around the band saw. Top half of frame and space between PVC and the band saw is wrapped in 6-mil polyethylene vapor barrier, forming an enclosure. All dimensions are in centimeters.

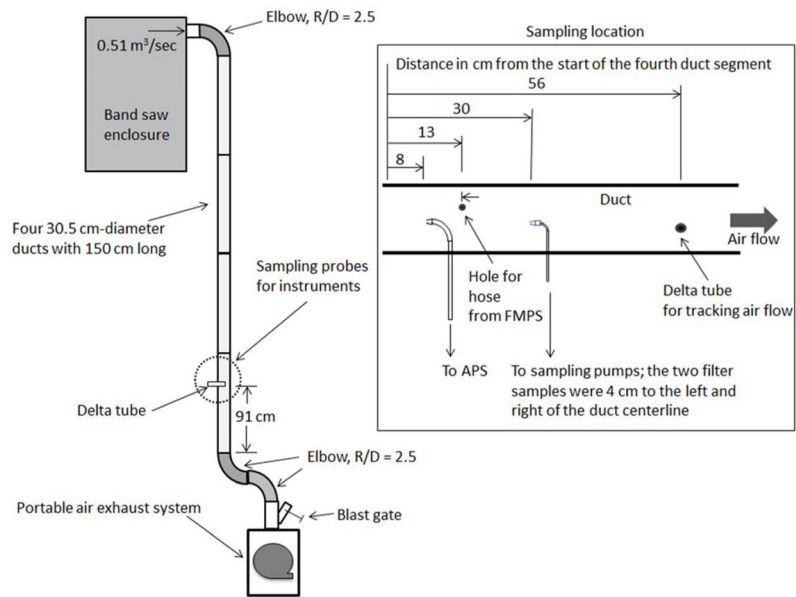


Figure 2. Plan view showing relationship between enclosure, duct, sampling locations and portable air exhaust system.



Figure 3.
Enclosed band saw.



Figure 4.
The sander at the inlet to the duct.

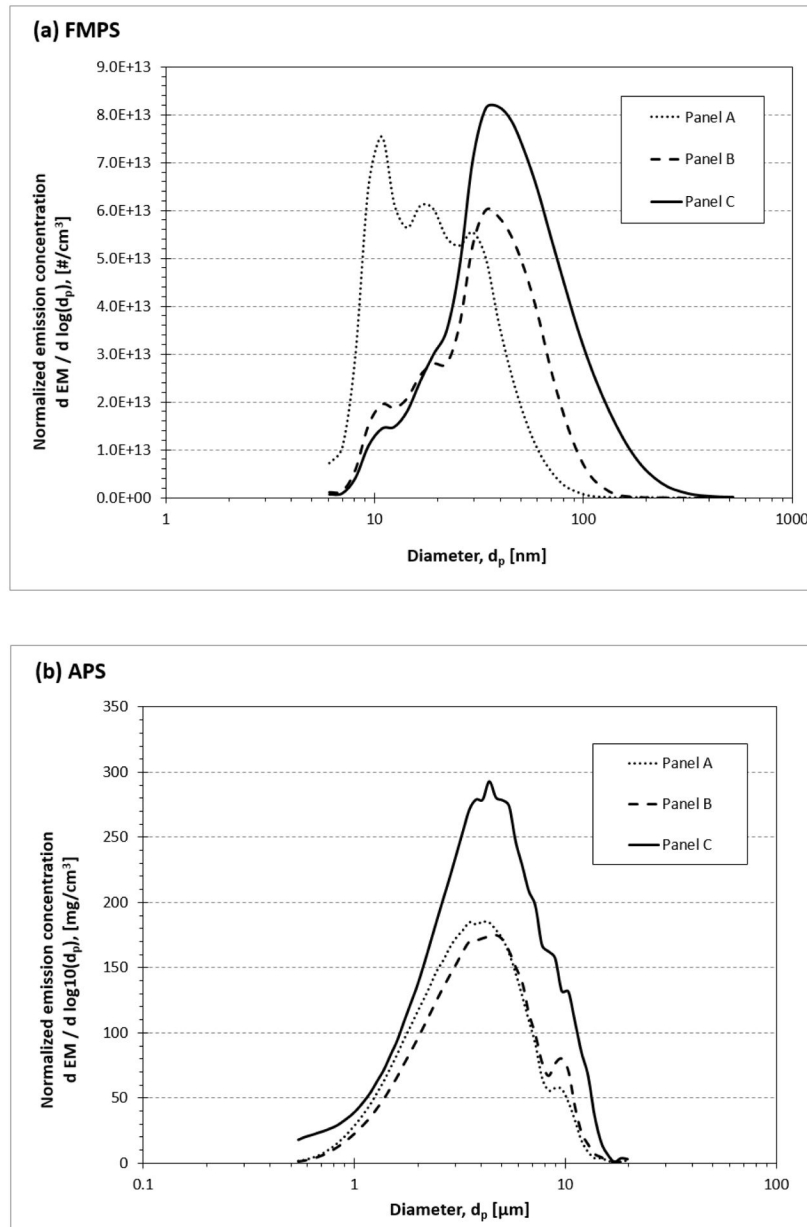


Figure 5. Size dependent emission rates based on (a) FMPS data and (b) APS data for cutting test panels.

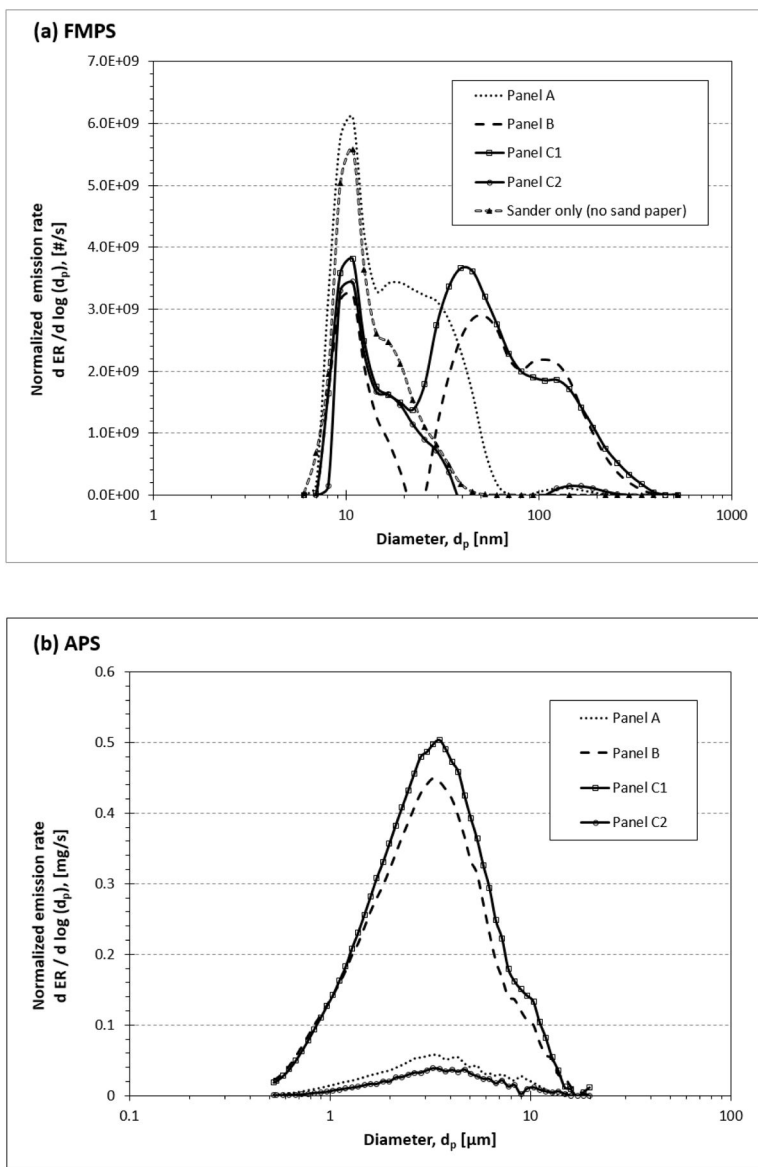


Figure 6. Size dependent emission rates based on (a) FMPS data and (b) APS data for sanding test panels.

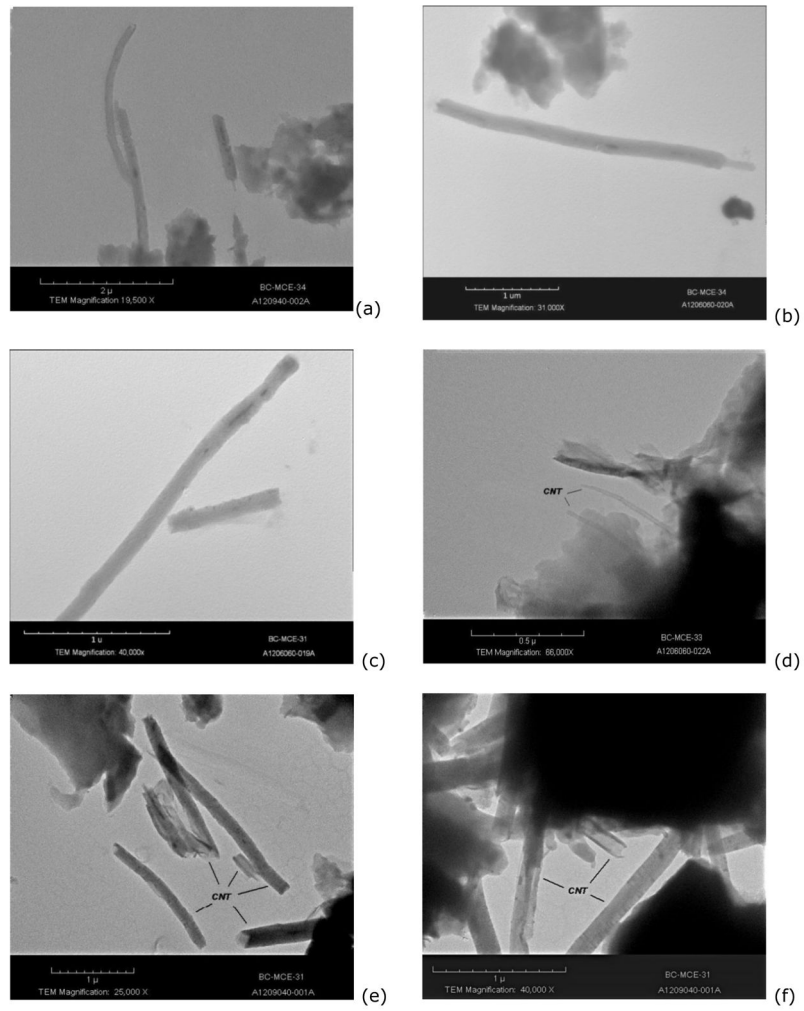


Figure 7.
TEM images of fibers generated from sanding Panel C containing CNTs.

Table 1

Provisional or draft exposure limit recommendations for engineered nanomaterials.

Description	Limit	Source of recommendation
Baytubes® MWCNTs	0.05 mg/m ³	(Bayer MaterialScience 2010)
CNTs measured as EC	1 µg/m ³ as an 8-hour TWA	(NIOSH 2013)
Nanocyl CNTs	2.5 µg/m ³	(Nanocyl 2009)
Biopersistent granular nanomaterials in the range of 1–100 nm with a density larger than 6000 kg/m ³	20,000 #/cm ³	Reference value for nanoparticles (van Broekhuizen et al. 2012; van Broekhuizen and Dorbeck-Jung 2013)
Biopersistent granular and fiber form nanomaterials in the range of 1–100 nm with density less than 6000 kg/m ³	40,000 #/cm ³	
Rigid, biopersistent nanofibres that have effects similar to those of asbestos are not excluded. This included carbon nanotubes.	0.01 f/cm ³ for fibers > 5 µm	

Author Manuscript

Author Manuscript

Author Manuscript

Author Manuscript

Table 2

Estimated aerosol transmission efficiencies for the APS and filter samples.

d_p (μm)	<u>Transmission efficiency</u>	
	APS	Filter samples
1	0.997	0.997
5	0.950	0.950
10	0.880	0.880

Author Manuscript

Author Manuscript

Author Manuscript

Author Manuscript

Table 3

Dimensions of the test panels and calculated volumes of cut (V_c) for the tests.

Test panel	Length x width (cm)	Thickness (cm)	V_c (cm ³)
A	30.5 × 30.5	0.21	3.106
B	30.5 × 30.5	0.45	6.787
C	30.5 × 30.5	0.28	2.292

Author Manuscript

Author Manuscript

Author Manuscript

Author Manuscript

Table 4

Summary of aerosol measurements and emission concentrations from cutting test panels.

Test Panel	FMPS			APS		
	C_n (#/cm ³)	EM (#/cm ³)	C_m (mg/m ³)	EM (mg/cm ³)	C_{resp}/C_m	
A	4.8E+05	4.6E+13	1.74	125	0.58	
B	7.3E+05	3.6E+13	2.56	120	0.53	
C	5.6E+05	5.5E+13	1.82	216	0.51	
Running Band saw without cutting	1.5E+04	-	0.05	-	-	
Background	1.1E+04	-	0.03	-	-	

Table 5

Results of filter sampling from cutting test panels.

Test Panel	EC concentration* ($\mu\text{g}/\text{m}^3$)			EC emission concentration based on volume of cut (mg/cm^3)
	Worker	Source	Duct	
A	0.3**	35	50	4.9
B	0.8**	93	84	4.1
C	< 0.7	54	75	6.9

* Background EC concentration = $1.8 \mu\text{g}/\text{m}^3$.

** between the LOD ($0.2 \mu\text{g}/\text{filter}$) and LOQ ($0.52 \mu\text{g}/\text{filter}$).

Table 6

Summary of aerosol measurements and emission rates from sanding test panels.

Test Panel	FMPS			APS		
	C_n (#/cm ³)	ER (#/s)	C_m (mg/m ³)	ER (mg/s)	C_{resp}/C_m	
A	1.7E+04	3.0E+09	0.101	0.040	0.60	
B	1.5E+04	3.6E+09	0.627	0.321	0.64	
C1	1.8E+04	4.3E+09	0.727	0.361	0.62	
C2	1.5E+04	1.0E+09	0.074	0.024	0.58	
Background	1.1E+04	–	0.028	–	–	
Sander alone	4.5E+03	2.0E+09	0.002	0.001	–	

Note: The in-duct sampling system was reassembled in our laboratory to evaluate the emissions from the sander alone (see Figure 4). The results were adjusted for different exhaust air flows.

Table 7

Summary of fiber concentrations detected by TEM during panel sanding.

Test Panel	Fiber concentration (f/cm ³)		Fiber emission rate (f/s)
	Source	Duct	
A	1 fiber detected	ND*	–
B	1 fiber detected	ND	–
C1	270	290	1.91×10 ⁸
C2	11	4.3	2.83×10 ⁶

* non-detectable if concentration less than 0.2 f/cm³. Fiber concentrations were below the LOD of 0.2 f/cm³ on the worker.

Table 8

Results of filter sampling from sanding test panels.

Test Panel	EC concentration* ($\mu\text{g}/\text{m}^3$)			EC emission rate based on sampling time ($\mu\text{g}/\text{s}$)
	Worker	Source	Duct	
A	0.80**	15.58	2.95	1.63
B	1.62	2.69	<0.4	< 0.22
C1	<0.5	7.50	3.85	2.51
C2	<0.5	<0.5	0.70**	0.39**

* Background EC concentration = $0.1 \mu\text{g}/\text{m}^3$.

** Between the LOD ($0.2 \mu\text{g}/\text{filter}$) and LOQ ($0.52 \mu\text{g}/\text{filter}$).